Second order finite volume methods with IMEX time-marching for linear and nonlinear parabolic PDE problems in option pricing[⋆]

J. G. López-Salas[a,∗], M. Suárez-Taboada[a], M. J. Castro[b], A. M. Ferreiro-Ferreiro[a], J. A. García-Rodríguez[a]

[a]*Department of Mathematics, Faculty of Informatics and CITIC, Campus Elviña s/n, 15071-A Coruña (Spain)*
[b]*Department of Análisis Matemático, Facultad de Ciencias, University of Málaga, Campus de Teatinos s/n, Málaga, 29080-Andalucía (Spain)*

Abstract

This article deals with the development of second order numerical schemes for solving option pricing problems, given by linear or nonlinear parabolic partial differential equations (PDEs), with nonlinearities in the source and/or convection terms. These equations will be discretized using second order finite volume Implicit-Explicit (IMEX) Runge-Kutta schemes. The here proposed numerical schemes have several advantages. First of all, they are able to reach high order, not only in the presence of nonregular initial conditions, the usual situation in finance, but also in the case of nonlinear advection and/or reaction terms, which appear in many recent and important PDEs in finance. Furthermore, the proposed schemes combine explicit and implicit time discretizations in a highly efficient way. They allow to take large time steps, overcoming the strict stability condition imposed for the diffusion terms in explicit schemes. Also,

the here proposed numerical schemes offer highly-accurate and non oscillatory approximations of option prices and their Greeks. Finally the developed numerical methods rely in a very general methodology, as they make use of well established techniques in the finite volume literature, such as numerical fluxes based in finite volume solvers, high order reconstruction operators or IMEX time marching schemes for stiff problems. This allows to apply these numerical schemes to a broad range of challenging state of the art problems in finance, given by nonlinear parabolic PDEs.

1. Introduction

In this article we present a general framework for building high-order finite volume numerical schemes for solving parabolic PDEs arising in option pricing. One important novelty is that the proposed numerical schemes are able to pre-
⁵ serve high-order, even in the case where the initial condition is not smooth, and without the need to regularize it. And even more important they are able to preserve high-order in nonlinear cases, where the advection and/or the source term are nonlinear, something which is not possible making use of fixed point schemes for the nonlinearities. Additionally, we show that that the obtained schemes only
¹⁰ need to comply with the convection CFL stability condition. Therefore, from the computational point of view, the here proposed schemes are orders of magnitude more efficient than explicit schemes. Thus, the here presented numerical schemes are able to solve very efficiently nonlinear PDEs, with special emphasis in semilinear PDEs and second-order quasilinear PDEs. These kinds of PDEs
¹⁵ are nowadays of paramount importance in mathematical finance, especially in the recent post financial crisis context of counterparty risk pricing and measurement, collateral and funding costs. On top of that, we are able to compute accurate and non oscillatory approximations of the derivatives of the numerical

solution, something which is much desirable in option pricing. Another important novelty of the work is that the here proposed numerical schemes profit from the use of all the well established finite volume tools for dealing with the convective terms at high-order: upwind of the convection is treated by means of numerical fluxes based on Riemann solvers, and well known state reconstruction operators are used for increasing the order of convergence.

To the best of our knowledge this is the first time this systematic framework is presented for building higher order schemes for solving nonlinear parabolic PDEs in option pricing.

Mathematical models for option pricing play a key role in the financial industry. An option is a contract that gives the right to buy or sell some underlying asset at a future date, for an agreed price. The price of the underlying asset is modelled via stochastic processes. These processes are described by stochastic differential equations (SDEs) or systems of SDEs. The value of an option at expiration is given by its payoff function. The expected present value of this payoff function is the option price before its maturity.

In the 1990s, the theory of backward SDEs (BSDEs) was initiated. BSDEs are SDEs for which a terminal condition is specified. El Karoui, Peng and Quenez proposed the first applications of BSDEs in finance in [1]. They proposed the so-called forward-backward SDEs (FBSDEs), consisting of a a backward SDE whose terminal condition is determined by the stochastic terminal value of the forward SDE. There are numerous and relevant applications of BSDEs in finance, see also [2].

Monte Carlo simulation is the straightforward choice for computing numerically the expectation defining the option price. This numerical method has many advantages. The fact that its order of convergence is independent of the dimension of the problem represents its major strength. Besides, the method allows to easily price options with sophisticated payoffs and complex models for the underlyings. Nevertheless, Monte Carlo simulation has also several drawbacks. Firstly, the method is very slow, since a large number of simulations are needed to get an accurate price. Secondly, the computation of derivatives of

option prices, the so-called Greeks, presents theoretical and practical challenges to Monte Carlo simulation. Besides, pricing barrier options by means of Monte Carlo simulation requires the use of the complex Brownian bridge techniques. Furthermore, the explicit evaluation of the nested conditional expectations appearing in FBSDEs is challenging and much more costly than the computation of plain expectations, see [3, 4]. Finally, note that the recent deep learning algorithms proposed to solve nonlinear PDEs (see [5] for example), although able to cope with the curse of dimensionality up to a certain extend, suffer form slow accuracy and huge computational costs.

Feynman-Kac formula establishes a connection between SDEs/FBSDEs and partial differential equations (PDEs). SDEs and linear BSDEs are linked to linear PDEs and nonlinear decoupled and coupled FBSDEs are connected with semilinear and quasilinear PDEs, respectively. Therefore, the option price can be computed by solving PDEs with classical numerical methods like finite differences, finite elements or finite volumes. Although these methods suffer the curse of dimensionality, they offer several advantages: solvers with high-order of convergence can be developed, the computation of the Greeks is straightforward, options in the nonlinear framework of FBSDEs can be naturally priced and exotic derivatives like barrier options fit very well in the PDE context, where only boundary conditions need to be changed. In this article we will develop deterministic numerical methods for solving Black-Scholes PDEs. These are advection-diffusion-reaction scalar PDEs, with the following general expression in dimension one

$$\frac{\partial u}{\partial t} + a(x,t)\frac{\partial u}{\partial x} + b(x,t)\frac{\partial^2 u}{\partial x^2} + H\left(x,t,u,\frac{\partial u}{\partial x}\right) = 0. \tag{1}$$

The discretization of these kind of financial PDEs for the linear cases with finite difference and finite element methods is discussed in [6, 7, 8, 9]. The combination of finite differences with Exponentially Fitted techniques is explained in [10]. Besides, Alternate Directions (ADI) with finite differences is illustrated in [11].

However, the development of finite difference and finite element numerical methods for PDEs arising in mathematical finance presents several well known

difficulties. First, and most important, these numerical methods usually show instabilities when the advection term becomes larger and/or the diffusion operator is degenerated. Upwinding techniques are needed to overcome this issue. Secondly, the development of high order pricers is challenging, because second order (or higher) convergence is lost when the initial condition is not regular: this is precisely the usual situation in option pricing, as the initial condition is given by a payoff function that is usually singular. Finally, another difficulty, derived from the previous ones, is achieving accurate and non oscillatory approximations of the Greeks. The derivatives of the solution are usually computed by means of finite difference formulas, which are very sensitive to small errors in the approximation of the prices. The higher the derivatives the more difficult is obtaining approximations without oscillations. This question is of paramount importance, since the Greeks are vital for trading purposes. Developing very accurate and high order schemes is a key step towards attaining non-fluctuating approximations of the Greeks.

In order to avoid the problems originated by non-smooth payoffs, smoothing techniques working on irregular initial data were proposed in the literature, see [12]. A commonly used smoothing technique is the so-called Rannacher's method, see [13]. It is well known that the second order Crank-Nicolson time marching scheme loses order when initial conditions are non-smooth, or the initial and boundary conditions are discontinuous, which is the situation with barrier options. Rannacher proposed a way to suppress wrongful initial oscillations, by preceding Crank-Nicolson with a few implicit steps.

Additionally, several numerical strategies were presented in the literature in order to overcome the problems emerging in convection dominated scenarios. One approach is the method of characteristics. In [14], Forsyth et al. solve option pricing problems with finite differences combined with the semi-Lagrangian characteristics method. In the finite element setup, semi-Lagrangian characteristics was applied in [15, 16] for pricing Asian options. In [17] the authors present a semi-Lagrangian finite difference method for pricing business companies. The main disadvantages of semi-Lagrangian methods in option pricing is the diffi-

culty to build high order numerical schemes. In fact, these numerical methods do not achieve second order convergence due to the non-smoothness of either the payoff or the boundary conditions. On top of that, the computational cost of characteristic method is high due to the demanding compulsory search at the foot of the characteristic and the required interpolation. Another approach for a better treatment of the advection terms is the use of finite volume methods. The first work applying finite volume methods in option pricing problems was [18]. Later, in [19] conservative explicit finite volume methods were proposed for convection dominated pricing problems. More precisely, the authors propose to use the extension of the central schemes presented by Nessyahu-Tadmor in [20] to the advection-diffusion problem developed in [21]. Recently, in [22], the authors propose a second order improvement to [19] with appropriate time methods and slope limiters. In [23] the authors apply the explicit third order Kurganov-Levy scheme presented in [24] along with the CWENO reconstructions presented in [25]. In all theses articles, it is shown that explicit finite volume schemes do not suffer loss in the order of convergence. Besides, they are able to obtain approximations of the Greeks without oscillations. Nevertheless, these works present numerical schemes explicit in time. Explicit time integrators introduce a severe restriction in the time step, imposed by the Von Neuman stability condition related to the diffusion terms. As a consequence, these schemes have a huge computational cost and are not able in practice to work with refined meshes in space, specially in problems with spatial dimension greater than one.

In this work we develop finite volume numerical solvers for option pricing problems. The proposed schemes address the mentioned problems of finite difference and finite element methods, while at the same time retain a large time step in the time discretization. More precisely, we present a general technique, following [26, 27], for building second-order Implicit-Explicit (IMEX) Runge-Kutta finite volume solvers for option pricing. This numerical scheme allows to use different numerical flux functions and opens the door to the consideration of high order reconstructions in mathematical finance. The proposed method is able to overcome the severe time step restriction thanks to the implicit treatment

of the diffusive part, while retaining at the same time the benefits of treating the advective term by means of a explicit finite volume scheme. In this way the stability condition of the IMEX scheme allows to use the same time step of the advective part, which is far larger than the diffusive time step. Moreover, finite volume schemes allow to address the loss of order of convergence when initial data is non-smooth, since they handle the integral version of the equations, working with the averaged solutions in each cell. Consequently, true second order schemes are proposed for option pricing problems, that also allow to recover accurate and non oscillatory approximations of the Greeks. Besides, IMEX schemes are particularly well suited for solving PDEs with nonlinear convection and or source terms, since they treat these terms explicitly while use implicit discretization only for the linear diffusion terms. This approach avoids either inefficient fixed point iterations or complex and less accurate linearization algorithms (see [28, 29] for example).

The organization of this paper is as follows. In the Section 2 we review Black-Scholes PDEs and vanilla, butterfly, barrier and Asian options. PDEs in the nonlinear credit valuation adjustment framework are also discussed. In Section 3 we describe the proposed finite volume IMEX Runge-Kutta numerical scheme. The extension of the method for nonlinear PDEs is also carried out. In Section 4, we present the numerical experiments that we have carried out. We validate the numerical scheme by pricing options with known analytical solution. More precisely, Section 4.1 is devoted to price vanilla, butterfly and barrier options under the classical Black-Scholes model. All these options are priced by means of solving the one dimensional Black-Scholes PDE with different terminal conditions. Besides, two nonlinear extensions of Black-Scholes PDE are also numerically solved. In Section 4.2 a two dimensional problem is considered: Asian options are valued by solving a two dimensional Black-Scholes PDE. Asian PDEs are solved by extending the one dimensional numerical schemes using the method of lines.

2. Option pricing PDE models

A financial derivative is a contract whose value depends on the evolution of the price of one or more assets, called underlying assets. An option is a kind of derivative consisting of a contract between two parties about trading a risky asset at a certain future time, or within a specified period of time, given by the exercise date or maturity (T). One party is the seller of the option, who fixes the terms of the contract, and gives to the option's holder the right (and not the obligation) to buy (call option) or sell (put option) a particular asset at a fixed price. This price is agreed on beforehand, and it is known as exercise price or strike (K).

Options are mainly characterized by the payoff function and the kind of allowed exercise. Call and put options, also called vanilla options, are the simplest ones. On the other hand, the so-called exotic options, have very complicated structures. An option is called path-dependent when its payoff depends explicitly on the values of the underlying asset at multiple dates before expiration. Examples of path dependent options are the barrier and Asian options. An option is called European if exercise is only permitted at maturity, and is called American if it can be exercised at any time before expiry.

Determining the fair price of the option, the so-called premium, at the time of the contract signature is an important financial problem. This is the subject of the present work. More precisely, we will focus on pricing several European-style options: vanilla options and exotic options (barrier and Asian options). For the dynamics of the underlying asset we will consider the Black-Scholes model, which is briefly introduced below.

2.1. Black-Scholes model

Let us now consider the Black-Scholes option pricing model presented in the articles by Merton [30] and Black and Scholes [31]. The model describes the evolution of the risky asset through the following SDE

$$\frac{ds_t}{s_t} = (r - q)dt + \sigma dW_t, \tag{2}$$

8

with W_t a standard Brownian motion. The parameter $r \in \mathbb{R}$ is the risk free constant interest rate and $q \in \mathbb{R}$ is the continuous dividend yield. This SDE implicitly describes the risk-neutral dynamics of the underlying asset price, since the coefficient on dt in (2), the so-called mean rate of return, is considered as $r - q$. The parameter $\sigma \in \mathbb{R}^+$ is the volatility of the stock price, which is again considered as constant. Black–Scholes model is based on several assumptions, like for example the fact that the volatility of the underlying asset is a deterministic constant (see [7] for details on all assumptions). Although nowadays all of these assumptions about the market can be shown wrong up to a certain extent, the Black-Scholes model is still very important in theory and practice, and it has a huge impact on financial markets.

The SDE (2) has analytical solution which can be expressed as

$$s_T = s_0 \exp\left(\left(r - q - \frac{1}{2}\sigma^2 \right) T + \sigma W_T \right),$$

where s_0 is the known current price of the underlying asset, and W_T is a random variable normally distributed with mean 0 and variance T. Therefore, the asset price has a lognormal distribution. For some payoffs, like those of vanilla options, the expected present value of the payoff of the option, which is an integral with respect to the lognormal density of s_T, can be analytically computed, giving rise to the celebrated Black-Scholes formulas for the prices of call and put options.

The price u of any option on the underlying s is fully determined at every instant t by the asset value s_t. Hence, the value of the option is a function $u(s,t)$. Applying Itô's lemma (see [32], for example), one can derive the SDE for u. In order to comply with the no-arbitrage conditions, the process du has to be martingale. Therefore, the drift term of the SDE for u must be zero, which implies the well-known linear parabolic backward in time Black-Scholes PDE

$$\frac{\partial u}{\partial t} + \frac{1}{2}\sigma^2 s^2 \frac{\partial^2 u}{\partial s^2} + (r-q)s\frac{\partial u}{\partial s} - ru = 0, \quad (s,t) \in [0,\infty) \times [0,T]. \tag{3}$$

Hereafter, in this work we will work forward in time by making the change of variable $\tau = T - t$ in (3). By abuse of notation this forward time τ is again

written as t, so that forward in time Black-Scholes PDE is

$$\frac{\partial u}{\partial t} - \frac{1}{2}\sigma^2 s^2 \frac{\partial^2 u}{\partial s^2} - (r-q)s\frac{\partial u}{\partial s} + ru = 0, \quad (s,t) \in [0,\infty) \times [0,T]. \quad (4)$$

PDE (4) must be completed with initial and boundary conditions. The initial condition $u(s,0)$ depends on the payoff of the option and the boundary conditions should be carefully determined taking into account financial aspects as well as mathematical questions. Throughout the next subsections several types of options will be described, together with their corresponding initial and boundary conditions.

2.1.1. Vanilla options

A European call option is the right to buy a risky asset at a fixed strike price K only at the future time T (measured in years). The call option holder would exercise the option at expiry if the asset price is above the strike K and not if it is below. Therefore, the payoff of a call option is $s_T - K$ if $s_T > K$ and 0 otherwise. Thus, the payoff of a European call option is $\max(s_T - K, 0)$. Conversely, a put option gives the right to sell. At expiry the option is worth $\max(K - s_T, 0)$. Therefore, the initial condition of (4) is $u(s,0) = \max(s - K, 0)$ for call options and $u(s,0) = \max(K - s, 0)$ for put options.

In order to solve numerically the Black-Scholes PDE we need to truncate the spatial domain. Therefore u will be computed for $s \in (0, \bar{s})$, with $\bar{s}$ large enough. Besides, boundary conditions have to be imposed at the boundaries. For call options the following Dirichlet boundary conditions can be used

$$u(0,t) = 0, \quad u(\bar{s},t) = \bar{s}e^{-qt} - Ke{-rt},$$

while for put options

$$u(0,t) = Ke{-rt} - \bar{s}e^{-qt}, \quad u(\bar{s},t) = 0.$$

The analytical solutions for European call and put options are given by (see [31, 30])

$$
\begin{aligned}
C(s,K,t) &= se^{-qt}N(d_1(s,K)) - Ke^{-rt}N(d_2(s,K)), \quad &(5)\\
P(s,K,t) &= Ke^{-rt}N(-d_2(s,K)) - se^{-qt}N(-d_1(s,K)), \quad &(6)
\end{aligned}
$$

where N is the cumulative distribution function of the standard normal distribution, and d_1, d_2 are defined as

$$d_1(s, K) = \frac{1}{\sigma\sqrt{t}}\left[\ln\left(\frac{s}{K}\right) + \nu t\right], \quad \nu = r - q + \frac{\sigma^2}{2}, \tag{7}$$

$$d_2(s, K) = d_1(s, K) - \sigma\sqrt{t}. \tag{8}$$

The delta of an option is the sensitivity of the option to a change in the underlying asset, $\Delta = \frac{\partial u}{\partial s}$. The gamma of an option, Γ, is the sensitivity of the delta to the underlying, $\Gamma = \frac{\partial^2 u}{\partial s^2}$. For call and put options under the Black-Scholes model, Greeks are known in closed form

$$\Delta_C(s, K, t) = e^{-qt}N(d_1(s, K)), \qquad \Gamma_C(s, K, t) = \frac{e^{-qt}n(d_1(s, K))}{s\sigma\sqrt{t}}, \tag{9}$$

$$\Delta_P(s, K, t) = -e^{-qt}N(-d_1(s, K)), \quad \Gamma_P(s, K, t) = \Gamma_C(s, K, t), \tag{10}$$

215 where $n(x) = \dfrac{e^{-x^2/2}}{\sqrt{2\pi}}$ is the probability density function of the standard normal distribution.

2.1.2. Butterfly spread

A butterfly spread is a financial product which involves buying two calls with strike prices K_1 and K_3 and selling two calls with strike price $K_2 = \frac{1}{2}(K_1 + K_3)$, where $K_1 < K_2 < K_3$. In this case, Black-Scholes PDE (4) is completed with the initial condition

$$u(s, 0) = \max(s - K_1, 0) + \max(s - K_3, 0) - 2\max\left(s - \frac{1}{2}(K_1 + K_3), 0\right),$$

and with homogeneous Dirichlet boundary conditions $u(0, t) = u(\bar{s}, t) = 0$.

The price of the butterfly spread is also known analytically and is given by

$$u(s, t) = C(s, K_1, t) + C(s, K_3, t) - 2C(s, K_2, t),$$

where C is the price of the call option given in (5). Thus, the Greeks of the
220 butterfly spread can be computed in closed form as a linear combination of the Greeks associated to the call options involved in the financial product.

11

2.1.3. Barrier options

Barrier options are exotic path-dependent options. One example of barrier options is the down-and-out call option. This derivative pays $\max(s - K, 0)$ at expiry, unless at any previous time the underlying asset touched or crossed a prespecified level B, called the barrier. In that situation the option becomes worthless. There are also *in* options which only pays off if the asset reached or crossed the barrier, otherwise they expire worthless. These barrier options are called continuously monitored barrier options.

A down-and-out call option under Black-Scholes model can be priced solving PDE (4) with initial condition

$$u(s, 0) = \begin{cases} \max(s - K, 0) & \text{for } s > B, \\ 0 & \text{for } s \leq B, \end{cases}$$

in the localized domain $(s, t) \in [B, \bar{s}] \times (0, T]$ with the boundary conditions $u(B, t) = 0$ and $u(\bar{s}, t) = se{-}qt - Ke{-}rt$ for $t \in (0, T]$. Due to the sharp discontinuity arising at the barrier this option is mathematically interesting in the PDE world. We will price this product with our proposed finite volume IMEX Runge-Kutta schemes.

Standard European continuously monitored barrier options can be priced in closed form. Their Greeks can be also computed analytically. In [30], Merton provides for first time such formulas. See also [33, 34, 35, 36]. Hereafter we are going to detail these formulas for down-and-in call options. Formulas for down-and-out call options can be inferred using that a portfolio consisting of an in option and its corresponding out option has the same price and Greeks of the corresponding vanilla option, i.e $C(s, K, t) = C_{DO}(s, K, t) + C_{DI}(s, K, t)$. All these formulas are needed in order to measure the accuracy and the order of convergence of the proposed numerical schemes. Greek formulas are carefully detailed below since we were not able to find them in the literature.

Let $\bar{K} = \max(B, K)$ and let $\lambda = \frac{2}{\sigma^2}(r - q - \frac{\sigma^2}{2})$. The price of the down-and-in

12

call option is given by:

$$C_{DI}(s, K, t) = \left(\frac{B}{s}\right)^\lambda \left[C\left(\frac{B^2}{s}, \bar{K}, t\right) + (\bar{K} - K)N\left(d_1\left(\frac{B^2}{s}, \bar{K}\right)\right)\right]$$
$$+ \left[P(s, K, t) - P(s, B, t) + \frac{(B - K)e^{-rt}}{\sigma s \sqrt{t}} N[-d_1(s, B)]\right] \mathbb{1}_{B>K} \quad (11)$$

Hereafter we compute the delta and the gamma Greeks for the down-and-in call option. In the following expressions, for sake of brevity, in the formulas of the prices and deltas of vanilla call and put options, the time t dependency is omitted. The delta of the down-and-in call option can be computed by deriving (11) with respect to s, and is given by

$$\Delta_{DI} = \frac{\Upsilon B^\lambda}{s^{\lambda+1}} + \left(\Delta_P(s, K) - \Delta_P(s, B) - \frac{(B - K)e^{-rt}}{\sigma s \sqrt{t}} n[-d_1(s, B)]\right) \mathbb{1}_{B>K}, \quad (12)$$

where

$$\Upsilon = - \lambda C\left[\frac{B^2}{s}, \bar{K}\right] - \frac{B^2}{s}\Delta_C\left[\frac{B^2}{s}, \bar{K}\right]$$
$$- (\bar{K} - K)e^{-rt}\left\{\lambda N\left[d_1\left(\frac{B^2}{s}, \bar{K}\right)\right] + \frac{1}{\sigma\sqrt{t}} n\left[d_1\left(\frac{B^2}{s}, \bar{K}\right)\right]\right\}.$$

Again, differentiating in (12) with respect to s, the gamma of the down-and-in call option is given by

$$\Gamma_{DI} = -\frac{\Upsilon B^\lambda(\lambda + 1)}{s^{\lambda+2}} + \frac{\Psi B^\lambda}{s^{\lambda+1}} +$$
$$\left[\Gamma_P(s, K) - \Gamma_P(s, B) + \frac{(B - K)e^{-rt}}{\sigma s^2 \sqrt{t}}\left(n[-d_1(s, B)] + \frac{1}{\sigma\sqrt{t}} n'[-d_1(s, B)]\right)\right] \mathbb{1}_{B>K}, \quad (13)$$

where

$$\Psi = \frac{B^2}{s^2}\left((\lambda + 1)\Delta_C\left[\frac{B^2}{s}, \bar{K}\right] + \frac{B^2}{s}\Gamma_C\left[\frac{B^2}{s}, \bar{K}\right]\right)$$
$$+ \frac{(\bar{K} - K)e^{-rt}}{\sigma s \sqrt{t}}\left(\lambda n\left[d_1\left(\frac{B^2}{s}, \bar{K}\right)\right] + \frac{1}{\sigma\sqrt{t}} n'\left[d_1\left(\frac{B^2}{s}, \bar{K}\right)\right]\right).$$

Finally, note that the delta and the gamma of the down-and-out call option can be obtained as $\Delta_{DO} = \Delta_C - \Delta_{DI}$ and $\Gamma_{DO} = \Gamma_C - \Gamma_{DI}$.

13

2.1.4. Asian options

Asian options are path dependent options whose payoff depends on the price s_T of the risky asset and also on the arithmetic average price a_T of the price s_t defined by $a_t = \frac{1}{t} \int_0^t s_\tau d\tau$. Different types of Asian options are traded in financial markets. Floating strike call options have the payoff function $\max(s_T - a_T, 0)$, while fixed strike call options consider the payoff $\max(a_T - K, 0)$, K being the strike price. American-style Asian options are also negotiated.

Let us denote by $u(s, a, t)$ the price of an Asian option. Under the standard Black-Scholes model for the risky asset, one can check that the price of an Asian option with payoff function $u_0(s, a)$ is the solution of the following forward in time two dimensional PDE (see [37])

$$\frac{\partial u}{\partial t} - \frac{1}{2}\sigma^2 s^2 \frac{\partial^2 u}{\partial s^2} - rs\frac{\partial u}{\partial s} - \frac{1}{T-t}(s-a)\frac{\partial u}{\partial a} + ru = 0, \quad u(s, a, 0) = u_0(s, a). \quad (14)$$

As an example, $u_0(s, a) = \max(a - K, 0)$ is the initial condition for an European fixed strike call option.

For European or American floating strike options, in [38] Ingersoll reduced PDE (14) to a one-dimensional PDE under a suitable change of variable. For European Asian options, both fixed and floating strike, in [39], Rogers and Shi showed that the value of the Asian option is governed by an alternative one dimensional PDE. Nevertheless, in order to value American-style fixed strike options, one can not use one dimensional models, and has to solve the two dimensional PDE (14). For this reason, in this work we restrict ourselves to the general two dimensional framework (14). Analytical solutions are not known, except for the case of fixed strike options with $K = 0$.

PDE (14) has no diffusion in the a variable, thus this equation is difficult to solve numerically. In fact, the convective term in the a direction increases as t approaches T. At $t = T$, PDE (14) has a singularity because of the $\frac{1}{T-t}(s-a)\frac{\partial u}{\partial a}$ term. For fixed strike options, the singularity can be avoided considering $s = a$ at $t = T$. Under this assumption, (14) reduces to Black-Scholes equation (4) at $t = T$.

In the Section 4 of the numerical experiments we will price a European-style

Asian fixed strike call option. PDE (14) will be solved in the localized domain $(s, a, t) \in (0, \bar{s}) \times (0, \bar{a}) \times (0, T]$ (usually $\bar{s} = \bar{a}$) with the following boundary condition $\frac{\partial^2 u}{\partial s^2}(\bar{s}, a, t) = 0$. The other portions of the boundary do not require the prescription of boundary conditions. Since the convective term in the a direction depends on time, once the problem is discretized, the matrices of the resulting systems have to be computed and inverted at each time step.

2.1.5. Counterparty risk

So far we have been dealing with linear PDEs. In this section we present two representative examples of semi-linear PDEs in finance. Firstly, in [40] the following PDE that models the value of the derivative including counterparty risk is presented:

$$\frac{\partial u}{\partial t} - \frac{1}{2}\sigma^2 s^2 \frac{\partial^2 u}{\partial s^2} - (r - q)s\frac{\partial u}{\partial s} + ru = -(1 - R_B)\lambda_B \min(u, 0)$$
$$- ((1 - R_C)\lambda_C + s_F) \max(u, 0), \quad (s, t) \in [0, \infty) \times (0, T], \qquad (15)$$

where B(buyer) and C(seller) are the two counterparties, R_B, $R_C \in [0, 1]$ represent recovery rates on derivatives positions of parties B and C, respectively, λ_B and λ_C are the default intensities and s_F is the funding cost of the entity.

Secondly, in [41], in the presence of initial margin, and assuming that the deposit is proportional to the CVaR of the portfolio over Δ days measured in years (typically one week, $\Delta \approx 0.02$) at the risk level α (typically $\alpha = 99\%$), the following pricing problem is presented

$$\frac{\partial u}{\partial t} - \frac{1}{2}\sigma^2 s^2 \frac{\partial^2 u}{\partial s^2} - rs\frac{\partial u}{\partial s} + ru - C_\alpha R\sigma\sqrt{\min(T - t + \Delta, T) - T + t}\left|s\frac{\partial u}{\partial s}\right| = 0,$$
$$(s, t) \in [0, \infty) \times (0, T],$$
$$(16)$$

with initial condition $u(s, 0) = \phi(s)$, $s \in \mathbb{R}^+$, where $C_\alpha = \mathbf{CVaR}^\alpha(\mathcal{N}(0, 1))$ and R is the interest rate determining the funding cost of the initial margin deposit. If the gradient $\dfrac{\partial u}{\partial s}$ has constant sign, the PDE (16) becomes linear and has an explicit solution given by the Black-Scholes formula with the following

time-dependent continuous dividend yield

$$q(t) = -C_\alpha R\sigma \sqrt{\min(T - t + \Delta, T) - T + t}\, \text{sign}\left(\frac{\partial u}{\partial s}\right)$$

$$= -C_\alpha R\sigma \sqrt{t\, \mathbf{1}_{t<\Delta} + \Delta\, \mathbf{1}_{t>=\Delta}}\, \text{sign}\left(\frac{\partial u}{\partial s}\right)$$

$$= -C_\alpha R\sigma \, \text{sign}\left(\frac{\partial u}{\partial s}\right) \times \begin{cases} \sqrt{t}, & t \in [0, \Delta], \\ \sqrt{\Delta}, & t \in [\Delta, T]. \end{cases}$$

Therefore, defining

$$Q(t) = -\int_0^t q(t)dt = -C_\alpha R\sigma \, \text{sign}\left(\frac{\partial u}{\partial s}\right)\left[\int_0^\Delta \sqrt{t}dt + \int_\Delta^t \sqrt{\Delta}dt\right]$$

$$= -C_\alpha R\sigma \, \text{sign}\left(\frac{\partial u}{\partial s}\right)\left[\frac{2}{3}\Delta^{\frac{3}{2}} + \sqrt{\Delta}(t - \Delta)\right],$$

the solution of the PDE (16) for call and put options is given by

$$C(s, K, t) = se^{-Q(t)}N(d_1(s, K)) - Ke^{-rt}N(d_2(s, K)), \qquad (17)$$

$$P(s, K, t) = Ke^{-rt}N(-d_2(s, K)) - se^{-Q(t)}N(-d_1(s, K)), \qquad (18)$$

where d_1, d_2 are defined as

$$d_1(s, K) = \frac{1}{\sigma\sqrt{t}}\left[\ln\left(\frac{s}{K}\right) + \nu t - Q(t)\right], \quad \nu = r + \frac{\sigma^2}{2}, \qquad (19)$$

$$d_2(s, K) = d_1(s, K) - \sigma\sqrt{t}. \qquad (20)$$

These analytical formulas, available only for plain derivatives, will allow us to accurately measure the order of convergence of the proposed numerical schemes.

3. Numerical methods. Finite volume IMEX Runge-Kutta

In this section we present a second order finite volume semi-implicit numerical scheme for solving (4). First, if possible, the equation (4) must be written in conservative form:

$$\frac{\partial u}{\partial t} + \frac{\partial}{\partial s}f(u, s) = \frac{\partial}{\partial s}g(u_s, s) + h(u). \qquad (21)$$

At the end of the section, for the PDE (16), which cannot be written in conservative form, a novel and ad-hoc numerical method for treating the nonlinearity be detailed. The numerical solution of equation (21) using a explicit finite volume scheme may have a huge computational cost because of the tiny time steps induced by the diffusive terms. To avoid this difficulty we consider IMEX Runge-Kutta methods (see [26]). These methods play a major rule in the treatment of differential systems governed by stiff and non stiff terms.

The procedure for obtaining the numerical scheme can be summarized as follows. First, we perform a spatial finite volume semi-discretization of (21), explicit in convection and reaction, and implicit in the diffusive part. As a result we obtain a stiff time ODE system, that we discretize using IMEX Runge-Kutta methods. In what follows we succinctly describe the space and time discretizations.

3.1. Spatial semi-discretization. Finite volume method

The spatial semi-discretization of the advective and source terms is performed by means of an explicit finite volume scheme. First, a finite volume mesh is built. The spatial domain is split into cells (finite volumes) $\{I_i\}$, with $I_i = [s_{i-1/2}, s_{i+1/2}]$, $i = \ldots, -1, 0, 1, \ldots$, being s_i the center of the cell I_i. Let $|I_i|$ be the size of cell I_i. The basic unknowns of our problem are the averages of the solution $u(s,t)$ in the cells $\{I_i\}$, $\bar{u}_i = \frac{1}{|I_i|} \int_{I_i} u \, ds$. Integrating equation (21) in space on I_i and dividing by $|I_i|$ we obtain the semi-discrete finite volume scheme

$$\frac{d\bar{u}_i}{dt} = -\frac{1}{|I_i|} \left(\mathcal{F}_{i+1/2}(t) - \mathcal{F}_{i-1/2}(t) \right) \tag{22}$$

$$+ \frac{1}{|I_i|} \left(\mathcal{G}_{i+1/2}(t) - \mathcal{G}_{i-1/2}(t) \right) \tag{23}$$

$$+ \frac{1}{|I_i|} \int_{I_i} h(\mathcal{R}^t(s)) \, ds. \tag{24}$$

In the previous expression, $\mathcal{F}_{i+1/2}(t)$ is a consistent numerical flux evaluated on the reconstructed states $u_{i+1/2}^{\pm}(t)$ at the intercell $s_{i+1/2}$. That is

$$u_{i\pm1/2}^{\pm}(t) = \lim_{s \to s_{i\pm1/2}^{\pm}} \mathcal{R}^t(s),$$

17

where $\mathcal{R}^t(s)$ is a reconstruction operator of the unknown function $u(s,t)$ defined in terms of the cell averages $\{\bar{u}_i(t)\}$, that could be written generally as

$$\mathcal{R}^t(s) = \sum_i P_i^t(s)\mathbb{1}_{s \in I_i},$$

where $P_i^t(s)$ is a reconstruction polynomial at cell I_i at time t satisfying some accuracy and non oscillatory properties, defined from the cell averages $\{\bar{u}_j(t)\}$ on a given stencil $j \in S_i$, and $\mathbb{1}_{s \in I_i}$ is the indicator function of cell I_i. For second order schemes, the reconstruction operator has to be at least piecewise linear. For example the left reconstructed value at the edge $s_{i+1/2}$ is

$$u_{i+1/2}^- = \bar{u}_i + \frac{1}{2}u_i',$$

where the slope u_i' is a first order approximation of the space derivative of $u(s,t)$ at point s_i at every time t. This slope must satisfy the TVD property and thus we must use slope limiters. In our case we use the minmod limiter, where the slope is given by

$$u_i' = \text{minmod}(\bar{u}_i - \bar{u}_{i-1}, \bar{u}_{i+1} - \bar{u}_i),$$

$$\text{minmod}(a,b) = \begin{cases} \min(a,b) & \text{if } a,b > 0, \\ \max(a,b) & \text{if } a,b < 0, \\ 0 & \text{otherwise}. \end{cases}$$

In this work $\mathcal{F}_{i+1/2}(t)$ is given by the CIR numerical flux

$$\mathcal{F}_{i+1/2} = \frac{1}{2}\left(f(u_{i+1/2}^-, s_{i+1/2}) + f(u_{i+1/2}^+, s_{i+1/2})\right) - \frac{\alpha_{i+1/2}}{2}\left(u_{i+1/2}^+ - u_{i+1/2}^-\right),$$

with

$$\alpha_{i+1/2} = \left| \frac{\partial f}{\partial u}\left(\frac{u_{i+1/2}^- + u_{i+1/2}^+}{2}\right) \right|. \tag{25}$$

In the previous expression we have dropped the time dependency for simplicity.

The integral of the source term (24) can be explicitly discretized using a quadrature rule. In this work, as we are interested on second order schemes we use the midpoint rule:

$$\int_{I_i} h(\mathcal{R}^t(s))ds \approx |I_i|\, h(\mathcal{R}^t(s_i)) = |I_i|\, h(\bar{u}_i). \tag{26}$$

18

Finally, $\mathcal{G}_{i+1/2}(t)$ is defined by

$$\mathcal{G}_{i+1/2} = g\left(\frac{\bar{u}_{i+1} - \bar{u}_i}{|I_i|}, s_{i+1/2}\right).$$

Again, we have dropped the time dependency for simplicity. Observe that $\frac{1}{|I_i|}\left(\mathcal{G}_{i+1/2} - \mathcal{G}_{i-1/2}\right)$ is a second order approximation of the diffusive term $\frac{\partial}{\partial s} g(u_s, s)$ at $s = s_i$.

3.1.1. Numerical method for PDE (16)

Equation (16) presents an extra difficulty due to the presence of the non-linear term $n(u_s, s) = b(t)\left|s\frac{\partial u}{\partial s}\right|$, with $b(t) = -C_\alpha R\sigma\sqrt{\min(T - t + \Delta, T) - T + t}$. Assuming that $s \in [0, \infty)$, $n(u_s, s)$ could be rewritten as $n(u_s, s) = sb(t)\mathrm{sign}\left(\frac{\partial u}{\partial s}\right)\frac{\partial u}{\partial s}$. Now, a discretization of this new term must be considered. Note that one could think that this term could be approximated as the standard source term $h(u)$, but this new term depends on u_s, so it must has a influence on the Riemann solver, in particular at the intercells where $u_{i+1/2}^- \neq u_{i+1/2}^+$. Moreover, this term has also an influence on the stability condition of the method. For these reasons, we propose the following semi-discrete finite volume scheme

$$
\begin{aligned}
\frac{d\bar{u}_i}{dt} = &-\frac{1}{|I_i|}\left(\mathcal{F}_{i+1/2}(t) - \mathcal{F}_{i-1/2}(t)\right) \\
&-\frac{1}{|I_i|}\left(\mathcal{N}_{i+1/2}(t) + \mathcal{N}_{i-1/2}(t)\right) - \frac{1}{|I_i|}\int_{I_i} n\left(\frac{\partial}{\partial s}\mathcal{R}^t(s), s\right)ds \quad (27) \\
&+\frac{1}{|I_i|}\left(\mathcal{G}_{i+1/2}(t) - \mathcal{G}_{i-1/2}(t)\right) \\
&+\frac{1}{|I_i|}\int_{I_i} h(\mathcal{R}^t(s))\,ds.
\end{aligned}
$$

As it could be seen, $n(u_s, s)$ introduces two different terms, one inside the cell, that corresponds to the integral of this term inside the cell I_i, and the terms $\mathcal{N}_{i\pm1/2}(t)$ that take into account the jumps of the unknown at the intercells $s_{i\pm1/2}$. As we are interested on second-order schemes, the integral term in (27) is approximated by the midpoint rule

$$\int_{I_i} n\left(\frac{\partial}{\partial s}\mathcal{R}^t(s), s\right)ds \approx |I_i|n\left(\frac{\partial}{\partial s}\mathcal{R}^t(s_i), s_i\right),$$

19

and the term $\mathcal{N}_{i+1/2}$ (similarly $\mathcal{N}_{i-1/2}$) is defined as

$$\mathcal{N}_{i+1/2} = \frac{1}{2} s_{i+1/2} b(t) \mathcal{S}_{i+1/2} \left(u_{i+1/2}^+ - u_{i+1/2}^- \right),$$

where $\mathcal{S}_{i+1/2}$ is an approximation of $\text{sign}(\frac{\partial u}{\partial s})$ at $s_{i+1/2}$. Here, we propose

$$\mathcal{S}_{i+1/2} = \frac{1}{2} (\text{sign}(s_{i+1/2} u_i' + \text{sign}(s_{i+1/2} u_{i+1}').$$

Again, in the previous expression we have dropped the time dependency for simplicity.

Note that the term $n(u_s, s)$ could be seen as a non-conservative term and the discretization proposed in (27) mimics the one proposed for non-conservative non-linear hyperbolic systems in [42]. We refer to [42] and the references therein for a detail description and justification of the numerical discretization proposed here.

Finally, let us remark that the presence of $n(u_s, s)$ also affects to the computation of $\alpha_{i+/2}$ in (25). In particular, for PDE (16) we use

$$\alpha_{i+1/2} = \left| \frac{\partial f}{\partial u} \left(\frac{u_{i+1/2}^- + u_{i+1/2}^+}{2} \right) + n \left(\frac{\partial}{\partial s} \mathcal{R}^t(s_{i+1/2}), s_{i+1/2} \right) \right|.$$

Note that $n(u_s, s)$ will also affect to the stability condition (33).

3.2. Time discretization. IMEX Runge-Kutta

After performing the spatial semi-discretization of equation (21) we obtain a stiff ODE system of the form

$$\frac{\partial U}{\partial t} + F(U) = S(U), \tag{28}$$

where $U = (\bar{u}_i(t))$ and $F, S : \mathbb{R}^N \to \mathbb{R}^N$, being F the non-stiff term and S the stiff one. An IMEX scheme consists of applying an implicit discretization to the stiff term and an explicit one to the non stiff term. In this way, both can be solved simultaneously with high order accuracy using the same *time step* of the convective part, which is in general much larger than the time step of the diffusive part.

20

When IMEX is applied to system (28) it takes the form

$$U^{(k)} = U^n - \Delta t \sum_{l=1}^{k-1} \tilde{a}_{kl} F(t_n + \tilde{c}_l \Delta t, U^{(l)}) + \Delta t \sum_{l=1}^{\rho} a_{kl} S(t_n + c_l \Delta t, U^{(l)}),$$

(29)

$$U^{n+1} = U^n - \Delta t \sum_{k=1}^{\rho} \tilde{\omega}_k F(t_n + \tilde{c}_k \Delta t, U^{(k)}) + \Delta t \sum_{k=1}^{\rho} \omega_k S(t_n + c_k \Delta t, U^{(k)}),$$

(30)

where $U^n = (\bar{u}_i^n)$, $U^{n+1} = (\bar{u}_i^{n+1})$ are the vector of the unknowns cell averages at times t^n and t^{n+1}, thus $U^{(k)}$ and U^l are the vector of unknowns at the stages k, l of the IMEX method. The matrices $\tilde{A} = (\tilde{a}_{kl})$, with $\tilde{a}_{kl} = 0$ for $l \geq k$, and $A = (a_{kl})$ are square matrices of order ρ, such that the ensuing scheme is implicit in S and explicit in F. Solving efficiently at each time step the system of equations corresponding to the implicit part is extremely important. Therefore, one usually considers $a_{kl} = 0$, for $l > k$, the so-called diagonally implicit Runge-Kutta (DIRK) schemes .

IMEX Runge-Kutta schemes can be represented by a double tableau in the usual Butcher notation,

$$\begin{array}{c|c} \tilde{c} & \tilde{A} \\ \hline & \tilde{\omega} \end{array}, \quad \begin{array}{c|c} c & A \\ \hline & \omega \end{array},$$

where $\tilde{w} = (\tilde{w}_1, \ldots, \tilde{w}_\rho)$ and $w = (w_1, \ldots, w_\rho)$. Besides, the coefficient vectors $\tilde{c} = (\tilde{c}_1, \ldots, \tilde{c}_\rho)^T$ and $c = (c_1, \ldots, c_\rho)^T$ are only used for the treatment of non autonomous systems, and have to satisfy the relations

$$\tilde{c}_k = \sum_{l=1}^{k-1} \tilde{a}_{kl}, \quad c_k = \sum_{l=1}^{k} a_{kl}.$$

(31)

In this work we will consider the second order IMEX-SSP2(2,2,2) L-stable scheme (see [26])

$$\begin{array}{c|cc} 0 & 0 & 0 \\ 1 & 1 & 0 \\ \hline & 1/2 & 1/2 \end{array} \quad \begin{array}{c|cc} \gamma & \gamma & 0 \\ 1-\gamma & 1-2\gamma & \gamma \\ \hline & 1/2 & 1/2 \end{array} \quad \gamma = 1 - \frac{1}{\sqrt{2}}.$$

21

An explicit time integrator needs extremely small time steps due to the following stability conditions

$$\eta \frac{\Delta t}{(\Delta s)^2} \leq \frac{1}{2},$$
(32)

$$\alpha \frac{\Delta t}{\Delta s} \leq 1,$$
(33)

where $\eta = \left| \dfrac{\partial g}{\partial u_s} \right|$, $\alpha = \left| \dfrac{\partial f}{\partial u} \right|$, for all cells I_i and for all boundary points $s_{i \pm 1/2}$. However, IMEX only needs to satisfy the advection stability condition (33).

4. Numerical experiments

In this section the accuracy and convergence of the proposed numerical scheme is assessed. The developed numerical method is applied to the discretization and solution of the one and two dimensional financial PDEs discussed in Section 2. More precisely, experiments under the linear and nonlinear Black-Scholes models for vanilla, butterfly and barrier options are presented in Section 4.1. Besides, the numerical results are compared with the analytical solutions presented in Section 2. Later, in Section 4.2 two dimensional problems in space are solved. Indeed, Asian options are priced.

At each one of the following subsections, we start by writing the involved PDE in conservative form. Then, graphs containing numerical results, such as option prices, Greeks (Delta and Gamma) and numerical errors are presented. Moreover, tables for the L_1 errors and the L_1 orders of convergence are shown. Additionally, a comparison of the time step sizes supplied by the stability conditions of the explicit and IMEX Runge-Kutta methods is presented. For all the tests in this paper a CFL of 0.5 is considered in the stability conditions.

4.1. Options under the Black-Scholes model

First of all, the Black-Scholes PDE (4) is written in the conservative form (21), where the conservative functions are given by:

$$f(u) = (\sigma^2 - r + q)su, \quad g(u_s) = \frac{1}{2}\sigma^2 s^2 \frac{\partial u}{\partial s}, \quad h(u) = (\sigma^2 - 2r + q)u.$$

22

Hereafter, vanilla, butterfly and barrier European call options are priced under this model.

4.1.1. European call options

In this section, three tests are considered, whose market data are collected in Table 1. Test 2 is a diffusion-dominated example, while Test 3 is convection-dominated. Test 1 represents a balanced configuration. Although the setup of Test 3 is financially unrealistic, because of the high value of r, it is useful as a stress-test of the numerical scheme. In these three experiments the spatial domain is set to $[0, \bar{s} = 400]$.

	σ	r	q	T	K
Test 1	0.01	0.10			
Test 2	0.5	0.02	0	1	100
Test 3	0.02	0.5			

Table 1: Market data for European call options under the Black-Scholes model.

In Figures 1, 2 and 3, numerical ($\bar{u}$) and exact (u) option prices are plotted at $t = T$ for Tests 1, 2 and 3, respectively. A mesh with 800 discretization points in space was considered. Numerical prices were computed with the IMEX Runge-Kutta time integrator. Besides, numerical errors ($|u - \bar{u}|$) are displayed in that figures. In addition, exact and numerical Delta and Gamma Greeks at the final time T are presented. The numerical Greeks ($\Delta\bar{u}$, $\Gamma\bar{u}$) are computed with second order finite differences approximations, even at the boundaries of the spatial domain, see [43] for details. The numerical results are plotted in red squares, while the analytical solutions are represented in continuous blue line. The reader can observe that the proposed finite volume numerical scheme offers high-resolution approximations, without oscillations, for the option prices and the Greeks, even at regions of discontinuities and non-smoothness in the initial condition.

Tables 2, 3 and 4 record L_1 errors and L_1 orders of convergence at $t = T$

23
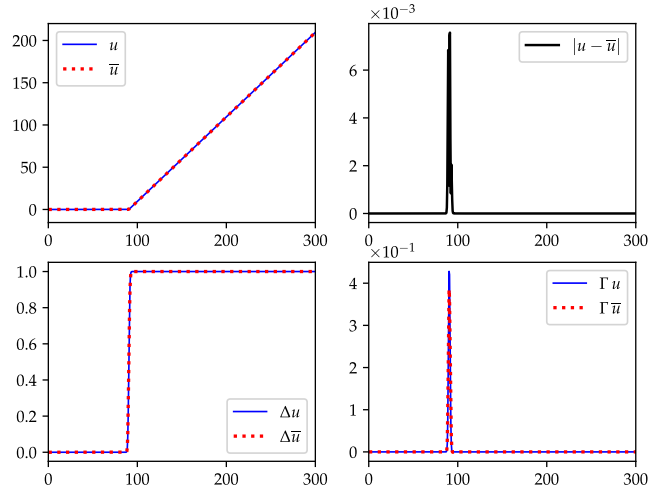
Figure 1: Call option prices, numerical errors and Greeks (Δ, Γ) for Test 1 at $t = T$.
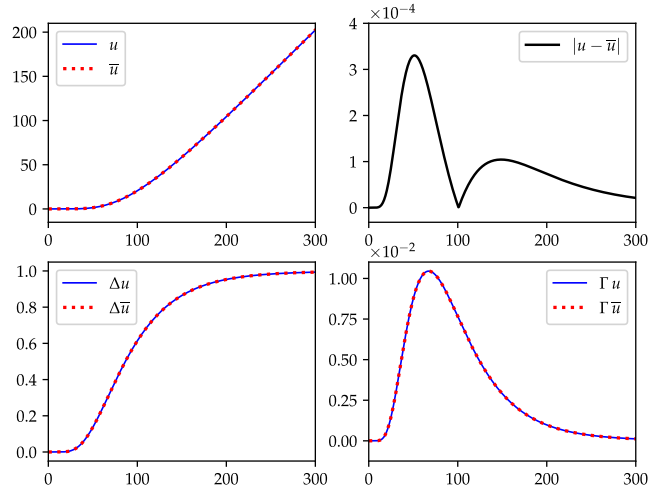
Figure 2: Call option prices, numerical errors and Greeks (Δ, Γ) for Test 2 at $t = T$.

for both explicit and IMEX finite volume numerical methods for Tests 1, 2
390 and 3, respectively. L_1 error is given by $L_1 = \Delta s \sum_{i=1}^{N} |\bar{u}(s_i, T) - u(s_i, T)|$,
where N denotes the number of discretization points in space. Besides, the
time steps and execution times are shown for each spatial discretization. The
time steps for IMEX and the explicit method were obtained from the stability
conditions (32) and (33). Codes were implemented using C++ programming

24
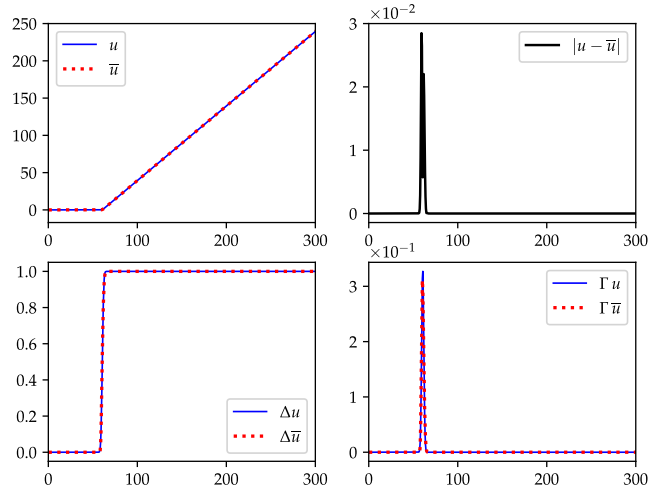
Figure 3: Call option prices, numerical errors and Greeks (Δ, Γ) for Test 3 at $t = T$.

language, compiled with GNU C++ compiler 9.3.0 and run in a machine with one AMD Ryzen 9 5950X processor. On the one hand, these tables show that both IMEX and explicit numerical schemes are able to approximate the solution with order two. Second order is achieved even in the presence of non-smoothness in the initial condition, thus avoiding the necessity of regularization techniques for the initial condition, like the Rannacher time-stepping. On the other hand, numerical results show, as expected, that the IMEX time integrator outperforms the explicit method. In fact, in the diffusion dominated scenario of Test 2, IMEX time steps are between 54 and 6967 times larger than corresponding explicit time steps. As a result, IMEX is between 17 and 1791 times faster than the explicit method. In Figure 4 the natural logarithms of L_1 errors and execution times of Table 3 are plotted for both the IMEX and explicit numerical schemes; IMEX superiority in this figure is overwhelming. As expected, when N increases the distance between both schemes is larger and larger. In advection dominated scenarios, like the one in Test 3, both IMEX and the explicit methods perform similarly in the coarser meshes in space. Nevertheless, IMEX performs again better when dealing with finer grids in space. For example, in the mesh with 6400 finite volumes, IMEX time step is 5 times larger than the corresponding

25

explicit time step, thus executing 1.64 times faster. In more balanced scenarios, like the one in Test 1, IMEX keeps performing better and better as long as the space grid is refined in space. In fact, in the grid with $N = 6400$, IMEX time step is 6.4 times larger than the explicit time step. As a result, IMEX is able to compute the solution 1.74 times faster. Having in mind that the common situation in finance is the diffusion dominated scenario, the IMEX time integrator represents the right choice. As a summary, although both time marching methods achieve similar results in terms of accuracy and convergence order, IMEX is able to converge using much larger times steps, thus it consumes much less computing time.

	IMEX			
N	L_1 error	Order	Δt	Time (s)
50	1.6145×10^1	$--$	1.01×10^{-1}	2.8×10^{-4}
100	7.1629×10^0	1.17	5.03×10^{-2}	4.7×10^{-4}
200	2.6877×10^0	1.41	2.50×10^{-2}	1.18×10^{-3}
400	9.1734×10^{-1}	1.55	1.25×10^{-2}	3.6×10^{-3}
800	2.8046×10^{-1}	1.70	6.26×10^{-3}	1.1×10^{-2}
1600	7.2788×10^{-2}	1.95	3.13×10^{-3}	2.6×10^{-2}
3200	1.7410×10^{-2}	2.06	1.56×10^{-3}	9.5×10^{-2}
6400	3.4791×10^{-3}	2.32	7.82×10^{-4}	3.5×10^{-1}

	Explicit			
N	L_1 error	Order	Δt	Time (s)
50	1.6146×10^1	$--$	1.01×10^{-1}	1.1×10^{-4}
100	7.1626×10^0	1.17	5.03×10^{-2}	1.9×10^{-4}
200	2.6875×10^0	1.41	2.50×10^{-2}	4.4×10^{-4}
400	9.1713×10^{-1}	1.55	1.25×10^{-2}	1.5×10^{-3}
800	2.8039×10^{-1}	1.71	6.26×10^{-3}	4.3×10^{-3}
1600	7.3346×10^{-2}	1.93	1.95×10^{-3}	2.2×10^{-2}
3200	1.7622×10^{-2}	2.06	4.88×10^{-4}	9.6×10^{-2}
6400	3.5252×10^{-3}	2.32	1.22×10^{-4}	6.1×10^{-1}

Table 2: L_1 errors and L_1 orders of convergence of the IMEX and explicit finite volume methods for the call option of Test 1.

4.1.2. Butterfly Spread

In this section a butterfly spread option is priced considering the market data $\sigma = 0.2$, $r = 0.1$, $q = 0$, $T = 0.5$, $K_1 = 45$ and $K_3 = 80$. The computational

26

	IMEX			
N	L_1 error	Order	Δt	Time (s)
50	7.8413×10^0	$--$	4.34×10^{-2}	3.8×10^{-4}
100	1.9886×10^0	1.98	2.17×10^{-2}	7.8×10^{-4}
200	5.0056×10^{-1}	1.99	1.09×10^{-2}	2.2×10^{-3}
400	1.2554×10^{-1}	1.99	5.43×10^{-3}	6.9×10^{-3}
800	3.1367×10^{-2}	2.00	2.72×10^{-3}	1.5×10^{-2}
1600	7.7625×10^{-3}	2.02	1.36×10^{-3}	5.0×10^{-2}
3200	1.8499×10^{-3}	2.07	6.80×10^{-4}	1.8×10^{-1}
6400	3.7004×10^{-4}	2.32	3.40×10^{-4}	6.7×10^{-1}
	Explicit			
N	L_1 error	Order	Δt	Time (s)
50	7.4158×10^0	$--$	8.00×10^{-4}	6.7×10^{-3}
100	1.8518×10^0	2.00	2.00×10^{-4}	1.8×10^{-2}
200	4.6253×10^{-1}	2.00	5.00×10^{-5}	8.7×10^{-2}
400	1.1551×10^{-1}	2.00	1.25×10^{-5}	4.8×10^{-1}
800	2.8793×10^{-2}	2.00	3.13×10^{-6}	2.9×10^0
1600	7.1211×10^{-3}	2.02	7.81×10^{-7}	2.0×10^1
3200	1.6999×10^{-3}	2.07	1.95×10^{-7}	1.5×10^2
6400	3.4735×10^{-4}	2.29	4.88×10^{-8}	1.2×10^3

Table 3: L_1 errors and L_1 orders of convergence of the IMEX and explicit finite volume methods for the call option of Test 2.
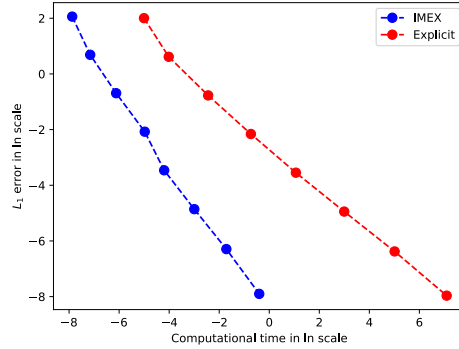

Figure 4: Efficiency curve of IMEX and explicit time marching schemes for Test 2.

domain is set as $[0, \bar{s} = 200]$.

In Figure 5, prices, numerical errors and Greeks are shown at $t = T$ with $N = 800$. These plots show that the here proposed numerical methods achieve very good approximations of prices and Greeks, even for this butterfly derivative,

	IMEX			
N	L_1 error	Order	Δt	Time (s)
50	3.4261×10^1	$--$	2.00×10^{-2}	5.8×10^{-4}
100	1.3092×10^1	1.39	1.00×10^{-2}	1.4×10^{-3}
200	4.8437×10^0	1.44	5.00×10^{-3}	4.4×10^{-3}
400	1.6448×10^0	1.56	2.50×10^{-3}	1.2×10^{-2}
800	4.8968×10^{-1}	1.75	1.25×10^{-3}	3.3×10^{-2}
1600	1.2745×10^{-1}	1.94	6.25×10^{-4}	1.1×10^{-1}
3200	3.0473×10^{-2}	2.06	3.13×10^{-4}	4.3×10^{-1}
6400	6.1026×10^{-3}	2.32	1.56×10^{-4}	1.7×10^0
	Explicit			
N	L_1 error	Order	Δt	Time (s)
50	3.4278×10^1	$--$	2.00×10^{-2}	3.5×10^{-4}
100	1.3124×10^1	1.39	1.00×10^{-2}	7.4×10^{-4}
200	4.8616×10^0	1.43	5.00×10^{-3}	1.9×10^{-3}
400	1.6535×10^0	1.56	2.50×10^{-3}	6.3×10^{-3}
800	4.9281×10^{-1}	1.75	1.25×10^{-3}	1.4×10^{-2}
1600	1.2841×10^{-1}	1.94	4.88×10^{-4}	5.3×10^{-2}
3200	3.0728×10^{-2}	2.06	1.22×10^{-4}	3.7×10^{-1}
6400	6.1716×10^{-3}	2.32	3.05×10^{-5}	2.8×10^0

Table 4: L_1 errors and L_1 orders of convergence of the IMEX and explicit finite volume methods for the call option of Test 3.

with sharp corners at strike prices in the initial condition and several jumps in derivatives. Second order of convergence is again achieved, although L_1 errors and L_1 orders of convergence are not shown for sake of brevity.

4.1.3. Barrier Option

In this section a down-and-out call option with the market data $\sigma = 0.2$, $r = 0.05$, $q = 0$, $T = 1$, $K = 70$ and the barrier at $B = 200$ is priced. The computational domain is thus set to $[B, 5B]$.

In Figure 6 option prices, numerical errors, Deltas and Gammas are shown at $t = T$ considering a mesh with $N = 800$. These plots show that the here proposed numerical methods are able to obtain good approximations without oscillations, even at difficult zones like close to the barrier. Table 5 shows L_1 errors and L_1 order of convergence at $t = T$. Second order accuracy is achieved again. In this case, IMEX time step is between 200 and 25606 times larger than
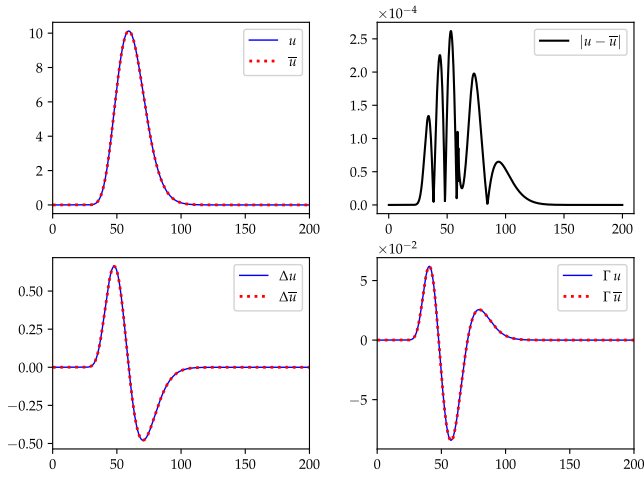
Figure 5: Butterfly spread option prices, numerical errors and Greeks (Δ, Γ).

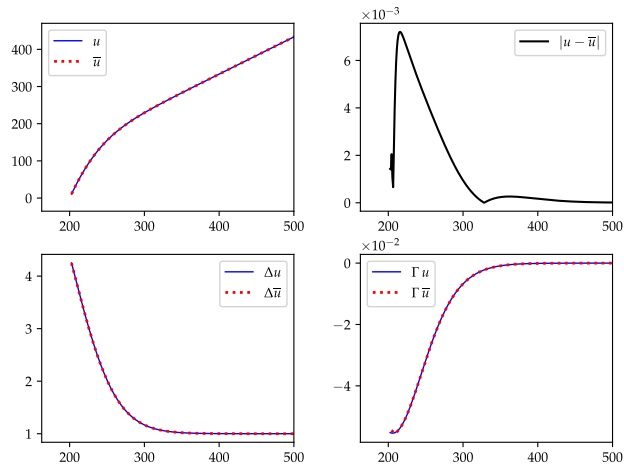the explicit time step. Consequently, IMEX executes between 10 and 12222 times faster.

Figure 6: Down-and-out call option prices, numerical errors and Greeks (Δ, Γ) at $t = T$.

29

| | IMEX | | | |
N	L_1 error	Order	Δt	Time (s)
50	1.3889×10^2	$--$	1.00×10^0	1.8×10^{-4}
100	3.4052×10^1	2.03	5.00×10^{-1}	2.6×10^{-4}
200	8.5310×10^0	2.03	2.50×10^{-1}	4.6×10^{-4}
400	2.1249×10^0	2.02	1.25×10^{-1}	9.4×10^{-4}
800	5.2912×10^{-1}	2.01	6.25×10^{-2}	2.4×10^{-3}
1600	1.3097×10^{-1}	1.98	3.13×10^{-2}	7.3×10^{-3}
3200	3.1547×10^{-2}	2.00	1.56×10^{-2}	1.6×10^{-2}
6400	6.7624×10^{-3}	2.26	7.81×10^{-3}	4.5×10^{-2}
	Explicit			
N	L_1 error	Order	Δt	Time (s)
50	1.3979×10^2	$--$	5.00×10^{-3}	1.8×10^{-3}
100	3.4401×10^1	2.02	1.25×10^{-3}	7.7×10^{-3}
200	8.5373×10^0	2.01	3.12×10^{-4}	3.0×10^{-2}
400	2.1271×10^0	2.01	7.81×10^{-5}	1.3×10^{-1}
800	5.3130×10^{-1}	2.01	1.95×10^{-5}	9.5×10^{-1}
1600	1.3316×10^{-1}	2.01	4.88×10^{-6}	6.4×10^0
3200	3.3721×10^{-2}	2.05	1.22×10^{-6}	6.4×10^1
6400	8.8809×10^{-3}	2.22	3.05×10^{-7}	5.5×10^2

Table 5: L_1 errors and L_1 orders of convergence of the IMEX and explicit finite volume methods for the down-and-out call option.

4.1.4. Counterparty credit risk

The PDE (15) is written in the conservative form (21), where the conservative functions are given by:

$$f(u) = (\sigma^2 - r + q)su, \quad g(u_s) = \frac{1}{2}\sigma^2 s^2 \frac{\partial u}{\partial s},$$

$$h(u) = (\sigma^2 - 2r + q)u - (1 - R_B)\lambda_B \min(u, 0) - ((1 - R_C)\lambda_C + s_F)\max(u, 0).$$

The market data is taken as $T = 5$, $K = 15$, $r = 0.02$, $\sigma = 0.3$, $q = 0$, $R_B = 0.4$, $R_C = 0.4$, $\lambda_B = \in \{0, 0.02, 0.04, 0.06, 0.08\}$, $\lambda_C = 0.05$ and $s_F = (1 - R_B)\lambda_B$. In Figures 7, 8 and 9 call option prices and Greeks are shown at $t = T$. Table 6 record L_1 errors and L_1 orders of convergence at $t = T$. The proposed numerical schemes continues to perform satisfactorily in this nonlinear setting.
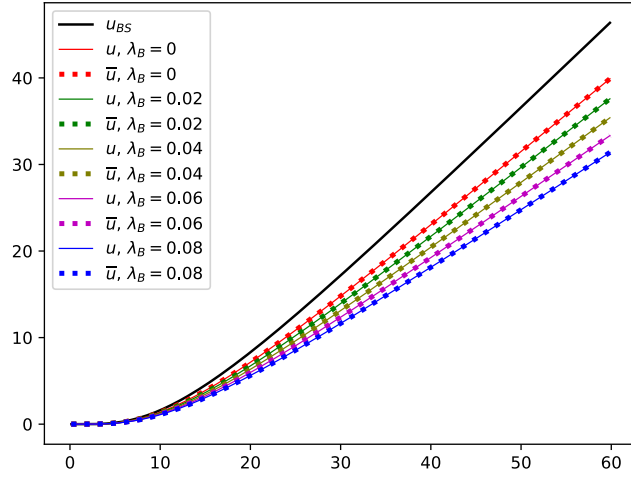
Figure 7: Call option prices with valuation adjustments at $t = T$. Exact value in continous line, numerical value with dots, for different values of the default intensities λ_B
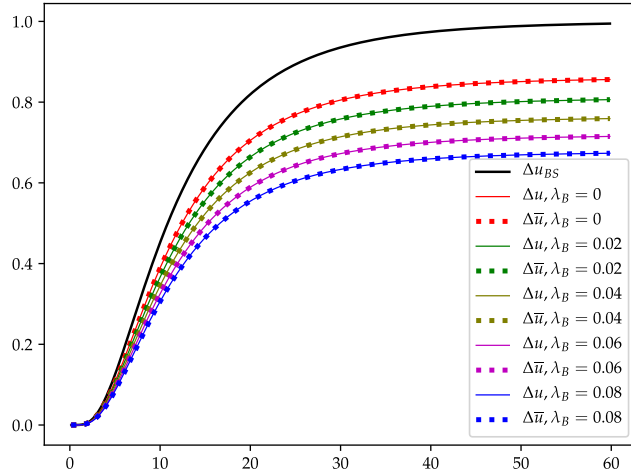
.

Figure 8: Δ with valuation adjustments at $t = T$. Exact value in continous line, numerical value with dots, for different values of the default intensities λ_B

4.1.5. Initial Margin problem

In this case the market data is taken as $T = 1.0$, $K = 20$, $r = 0.02$, $\sigma = 0.25$, $R = 0.02$, $\Delta = 0.02$ and $\alpha = 0.99$. In Figures 10, 11 and 12 call options prices
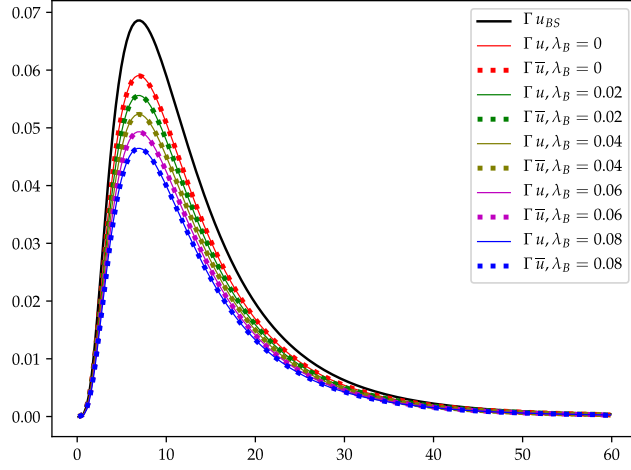
Figure 9: Γ with valuation adjustments at $t = T$. Exact value in continous line, numerical value with dots, for different values of the default intensities λ_B

	IMEX			
N	L_1 error	Order	Δt	Time (s)
50	1.4323×10^{-1}	$--$	1.44×10^{-1}	7.2×10^{-3}
100	3.6714×10^{-2}	1.96	7.17×10^{-2}	1.8×10^{-3}
200	9.2457×10^{-3}	1.99	3.58×10^{-2}	4.5×10^{-3}
400	2.3140×10^{-3}	2.00	1.78×10^{-2}	1.1×10^{-2}
800	5.7768×10^{-4}	2.00	8.93×10^{-3}	2.4×10^{-2}
1600	1.4413×10^{-4}	2.00	4.46×10^{-3}	7.8×10^{-2}
3200	3.5943×10^{-5}	2.00	2.23×10^{-3}	2.7×10^{-1}
6400	8.9052×10^{-6}	2.01	1.11×10^{-3}	1.0×10^{0}
	Explicit			
N	L_1 error	Order	Δt	Time (s)
50	1.4255×10^{-1}	$--$	2.23×10^{-3}	1.2×10^{-2}
100	3.5607×10^{-2}	2.00	5.56×10^{-4}	1.7×10^{-2}
200	8.8734×10^{-3}	2.00	1.39×10^{-4}	8.3×10^{-1}
400	2.2145×10^{-3}	2.00	3.47×10^{-5}	3.8×10^{0}
800	5.5312×10^{-4}	2.00	8.68×10^{-6}	2.2×10^{1}
1600	1.3823×10^{-4}	2.00	2.17×10^{-6}	8.7×10^{1}
3200	3.4467×10^{-5}	2.00	5.42×10^{-7}	7.3×10^{2}
6400	8.6169×10^{-6}	2.00	1.36×10^{-7}	3.5×10^{3}

Table 6: L_1 errors and L_1 orders of convergence of the IMEX and explicit finite volume methods for the call with valuation adjustments.

and Greeks are shown at $t = T$. Also in this case, the proposed numerical scheme achieves second order accuracy even for this PDE with a complicated non-linear term. The table with errors and order of convergence is not shown here just for sake of brevity. The considered boundary conditions were homogeneous Dirichlet on the left, and $\dfrac{\partial^2 u}{\partial s^2} = 0$ on the right. Such so-called linear boundary condition is important in order to avoid the so-called order reduction issue appearing when time dependent boundary conditions are considered along with IMEX time marching schemes.
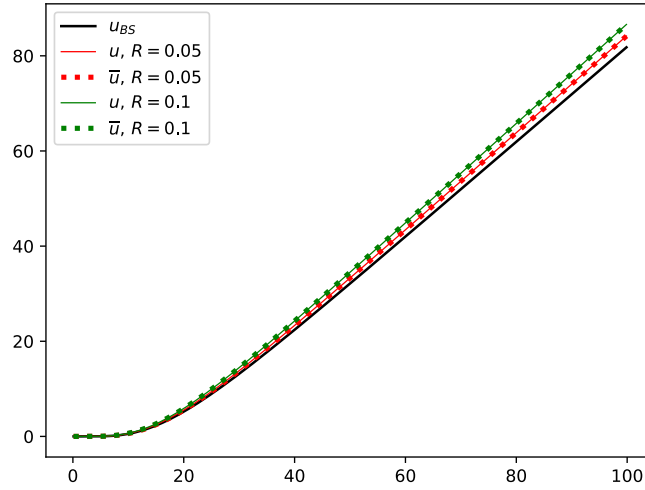

Figure 10: Call option prices considering initial margin at $t = T$. Exact value in continous line, numerical value with dots, for different values of the financing interest rate.

.

4.2. Asian option

Using the method of lines, the previous one dimensional numerical methods can be easily extended to the two dimensional case. Generally speaking, we are interested in solving the following two dimensional advection-diffusion-reaction PDE:

$$\frac{\partial u}{\partial t} + a\frac{\partial u}{\partial x} + b\frac{\partial u}{\partial y} + c\frac{\partial^2 u}{\partial x^2} + d\frac{\partial^2 u}{\partial y^2} + e = 0 \,, \tag{34}$$
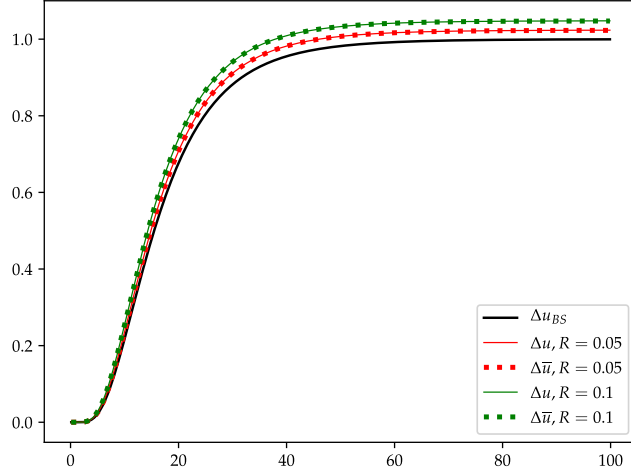
33

Figure 11: Δ considering initial margin at $t = T$. Exact value in continous line, numerical value with dots, for different values of the financing interest rate.
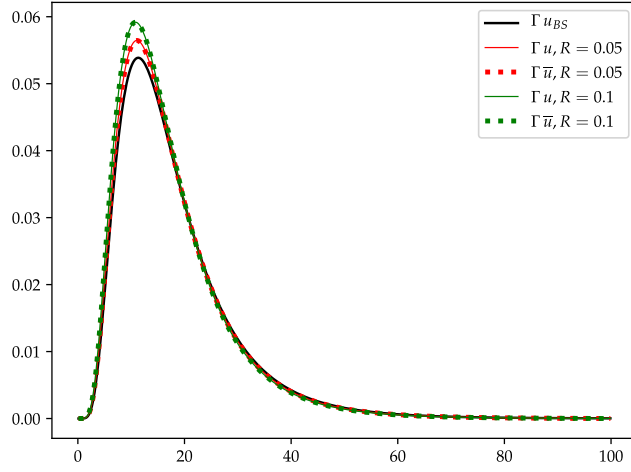

Figure 12: Γ considering initial margin at $t = T$. Exact value in continous line, numerical value with dots, for different values of the financing interest rate.

where a, b, c, d, e are functions of t, x, y and u. This equation (34) can be written in conservative form as

$$\frac{\partial u}{\partial t} + \frac{\partial f_1}{\partial x}(u) + \frac{\partial f_2}{\partial y}(u) = \frac{\partial g_1}{\partial x}(u_x) + \frac{\partial g_2}{\partial y}(u_y) + h(u). \tag{35}$$

34

The stability conditions are

$$2\eta_1 \frac{\Delta t}{(\Delta x)^2} + 2\eta_2 \frac{\Delta t}{(\Delta y)^2} \leq \frac{1}{2}, \quad \alpha_1 \frac{\Delta t}{\Delta x} + \alpha_2 \frac{\Delta t}{\Delta y} \leq 1, \tag{36}$$

where $\eta_1 = \left|\frac{\partial g_1}{\partial u_x}\right|$, $\eta_2 = \left|\frac{\partial g_2}{\partial u_y}\right|$, $\alpha_1 = \left|\frac{\partial f_1}{\partial u}\right|$ and $\alpha_2 = \left|\frac{\partial f_2}{\partial u}\right|$ for all boundaries of all volumes.

Therefore, the Asian PDE (14) is then written in the conservative form of PDE (35) using

$$
\begin{aligned}
f_1(u) &= (\sigma^2 - r)su, \quad f_2(u) = -\frac{1}{T-t}(s-a)u, \\
g_1(u_s) &= \frac{1}{2}\sigma^2 s^2 u_s, \quad g_2(u_a) = 0, \quad h(u) = \left(\sigma^2 - 2r + \frac{1}{T-t}\right)u.
\end{aligned}
$$

At this point, a fixed strike Asian call option is valued with the market data $\sigma = 0.2$, $r = 0.1$, $T = 1$, $K = 100$ on the spatial domain $(s, a) \in [0, 300] \times [0, 300]$. Numerical option prices and Greeks at $t = T$ using a mesh of size $N_1 \times N_2 = 800 \times 800$ are shown in Figure 13.

Table 7 records L_1 errors and L_1 orders of convergence at $t = \frac{T}{2}$. Both IMEX and explicit numerical schemes achieve second-order accuracy in the L_1 norm. In this case f_2 depends on time t. Therefore, the time step inferred by the convective stability condition in (36) depends on the actual time step. For each row of the table, only the smallest time step is shown, i.e the one computed at the final time step. In the case of this financial derivative, IMEX time marching is up to 40 times faster than the explicit scheme.

5. Conclusions

In this article we have shown that finite volume IMEX Runge-Kutta numerical schemes are remarkably suitable for solving PDE option pricing problems. On the one hand, the IMEX time discretization is remarkably efficient. Indeed, large time steps can be used, avoiding the need to use the smaller, and possibly extremely small, time steps enforced by the diffusion stability condition, which has to be satisfied in explicit schemes. Numerical results show that IMEX outperforms the explicit method. In fact, IMEX is the only way to solve problems

35
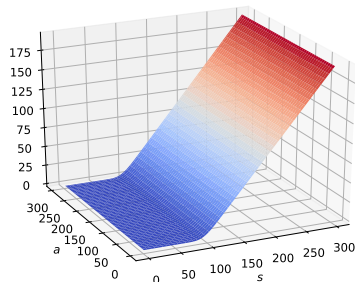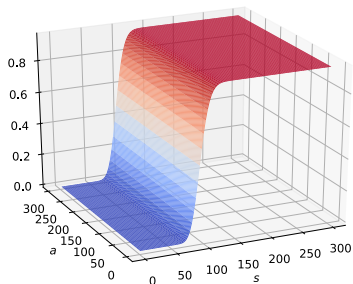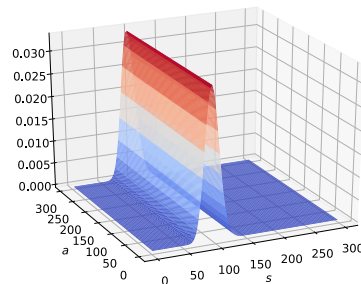
(a) Price.

(b) Delta.

(c) Gamma.

Figure 13: Prices, Deltas and Gammas of the Asian option at $t = T$.

in highly refined meshes is space. Besides, even in its worst scenarios, IMEX performs at least as well as the explicit method. On the other hand, finite volume space discretization contributes substantially to the achievement of second order convergence. Its consideration is crucial to handle appropriately con-
490   vection dominated problems and/or problems with non smooth initial and/or boundary conditions, which is the usual situation in finance. Thus, no special regularization techniques of the non smooth data need to be taken into account. The accuracy of the numerical scheme turns to be of key importance for the accurate and non oscillatory computation of the Greeks. Finally, in this paper we
495   provide a set of benchmark problems, together with their analytical solutions. These benchmarks can also be valuable for mathematical researchers working in the development of high order numerical schemes for advection-diffusion problems.

36

	IMEX			
$N_1 \times N_2$	L_1 error	Order	Δt	Time (s)
25×25	2.6092×10^4	$--$	1.00×10^{-2}	1.7×10^{-2}
50×50	8.5678×10^3	1.61	5.00×10^{-3}	8.0×10^{-2}
100×100	8.5678×10^3	1.42	2.50×10^{-3}	5.9×10^{-1}
200×200	1.2092×10^3	1.40	1.25×10^{-3}	5.7×10^0
400×400	3.2323×10^2	1.90	6.25×10^{-4}	5.3×10^1
800×800	9.7991×10^1	1.72	3.13×10^{-4}	5.1×10^2
1600×1600	2.3879×10^1	2.04	1.57×10^{-4}	5.0×10^3
	Explicit			
$N_1 \times N_2$	L_1 error	Order	Δt	Time (s)
25×25	2.6273×10^4	$--$	1.00×10^{-2}	8.1×10^{-3}
50×50	8.5704×10^3	1.62	5.00×10^{-3}	3.5×10^{-2}
100×100	2.9837×10^3	1.52	1.25×10^{-3}	2.3×10^{-1}
200×200	9.8509×10^2	1.59	3.12×10^{-4}	4.1×10^0
400×400	3.2357×10^2	1.61	7.81×10^{-5}	6.6×10^1
800×800	9.8241×10^1	1.72	1.95×10^{-5}	1.2×10^3
1600×1600	2.4234×10^1	2.02	4.88×10^{-6}	2.0×10^5

Table 7: L_1 errors and L_1 orders of convergence of the IMEX and explicit finite volume methods for the Asian option.

References

[1] N. E. Karoui, S. Peng, M. C. Quenez, Backward Stochastic Differential Equations in Finance, Mathematical Finance 7 (1) (1997) 1–71.

[2] S. Crepey, Financial modeling: a backward stochastic differential equations perspective, Springer, 2013.

[3] E. Gobet, J. G. López-Salas, P. Turkedjiev, C. Vázquez, Stratified Regression Monte-Carlo Scheme for Semilinear PDEs and BSDEs with Large Scale Parallelization on GPUs, SIAM Journal on Scientific Computing 38 (6) (2016) C652–C677.

[4] E. Gobet, J. G. López-Salas, C. Vázquez, Quasi-Regression Monte-Carlo Scheme for Semi-Linear PDEs and BSDEs with Large Scale Parallelization on GPUs, Archives of Computational Methods in Engineering 27 (2020) 889–921.

[5] Jiequn Han and Arnulf Jentzen and Weinan E, Solving high-dimensional partial differential equations using deep learning, Proceedings of the National Academy of Sciences 115 (34) (2018) 8505–8510.

[6] D. Duffy, Finite Difference Methods in Financial Engineering: A Partial Differential Equation Approach, Wiley, 2006.

[7] P. Wilmott, Paul Wilmott on Quantitative Finance, Wiley, 2006.

[8] Y. Achdou, O. Pironneau, Frontiers in Applied Mathematics. Computational Methods for Option Pricing, SIAM, 2005.

[9] A. Pascucci, PDE and Martingale Methods in Option Pricing, Springer, 2011.

[10] D. J. Duffy, Exponentially fitted difference schemes for barrier options, in: Finite Difference Methods in Financial Engineering: A Partial Differential Equation Approach, John Wiley & Sons, Ltd, 2013, Ch. 14, pp. 153–163.

[11] K. J. I. T. Hout, S. Foulon, ADI finite difference schemes for option pricing in the Heston model with correlation, International Journal of Numerical Analysis and Modeling 7 (2) (2010) 303–320.

[12] B. Wade, A. Khaliq, M. Yousuf, J. Vigo-Aguiar, R. Deininger, On smoothing of the Crank–Nicolson scheme and higher order schemes for pricing barrier options, Journal of Computational and Applied Mathematics 204 (1) (2007) 144 – 158.

[13] M. Luskin, R. Rannacher, W. Wendland, On the Smoothing Property of the Crank-Nicolson scheme, Applicable Analysis 14 (2) (1982) 117–135.

[14] Y. d'Halluin, P. A. Forsyth, G. Labahn, A Semi-Lagrangian Approach for American Asian Options under Jump Diffusion, SIAM Journal on Scientific Computing 27 (1) (2006) 315–345.

[15] A. Bermúdez, M. R. Nogueiras, C. Vázquez, Numerical analysis of convection-diffusion-reaction problems with higher order characteristics finite elements. Part I: Time discretization, SIAM Journal on Numerical Analysis 44 (5) (2006) 1829–1853.

[16] A. Bermúdez, M. R. Nogueiras, C. Vázquez, Numerical solution of variational inequalities for pricing asian options by higher order lagrange–galerkin methods, Applied Numerical Mathematics 56 (10) (2006) 1256–1270.

[17] D. Castillo, A. Ferreiro, J. García-Rodríguez, C. Vázquez, Numerical methods to solve PDE models for pricing business companies in different regimes and implementation in GPUs, Applied Mathematics and Computation 219 (24) (2013) 11233 – 11257.

[18] R. Zvan, P. A. Forsyth, K. R. Vetzal, A finite volume approach for contingent claims valuation, IMA Journal of Numerical Analysis 21 (3) (2001) 703–731.

[19] G. I. Ramírez-Espinoza, M. Ehrhardt, Conservative and Finite Volume Methods for the Convection-Dominated Pricing Problem, Advances in Applied Mathematics and Mechanics 5 (6) (2013) 759–790.

[20] H. Nessyahu, E. Tadmor, Non-oscillatory central differencing for hyperbolic conservation laws, Journal of Computational Physics 87 (2) (1990) 408–463.

[21] A. Kurganov, E. Tadmor, New high-resolution central schemes for nonlinear conservation laws and convection–diffusion equations, Journal of Computational Physics 160 (1) (2000) 241 – 282.

[22] O. Bhatoo, A. A. I. Peer, E. Tadmor, D. Y. Tangman, A. A. E. F. Saib, Efficient conservative second-order central-upwind schemes for option-pricing problems, Journal of Computational Finance 22 (5) (2019) 39–78.

[23] O. Bhatoo, , A. A. I. Peer, E. Tadmor, D. Y. Tangman, A. A. E. F. Saib, Conservative third-order central-upwind schemes for option pricing problems, Vietnam Journal of Mathematics 47 (4) (2019) 813–8332.

[24] A. Kurganov, D. Levy, A Third-Order Semidiscrete Central Scheme for Conservation Laws and Convection-Diffusion Equations, SIAM Journal on Scientific Computing 22 (4) (2000) 1461–1488.

[25] D. Levy, G. Puppo, G. Russo, Compact central WENO schemes for multidimensional conservation laws, SIAM Journal on Scientific Computing 22 (2) (2000) 656–672.

[26] L. Pareschi, G. Russo, Implicit–Explicit Runge–Kutta Schemes and Applications to Hyperbolic Systems with Relaxation, Journal of Scientific Computing 25 (2005) 129–155.

[27] S. Boscarino, G. Russo, On a Class of Uniformly Accurate IMEX Runge–Kutta Schemes and Applications to Hyperbolic Systems with Relaxation, SIAM Journal on Scientific Computing 31 (3) (2009) 1926–1945.

[28] I. Arregui, B. Salvador, D. Ševčovič, C. Vázquez, Total value adjustment for European options with two stochastic factors. Mathematical model, analysis and numerical simulation, Computers & Mathematics with Applications 76 (4) (2018) 725–740.

[29] M. A. Baamonde-Seoane, M. C. Calvo-Garrido, M. Coulon, C. Vázquez, Numerical solution of a nonlinear PDE model for pricing Renewable Energy Certificates (RECs), Applied Mathematics and Computation 404 (2021) 126199.

[30] R. C. Merton, Theory of Rational Option Pricing, The Bell Journal of Economics and Management Science 4 (1) (1973) 141–183.

[31] F. Black, M. Scholes, The Pricing of Options and Corporate Liabilities, The Journal of Political Economy 81 (3) (1973) 637–654.

[32] S. E. Shreve, Stochastic Calculus for Finance, Springer, 2004.

[33] M. Rubinstein, E. Reiner, Breaking down the barriers, Risk 4 (8) (1991) 28–35.

[34] D. Rich, The Mathematical Foundations of Barrier Option Pricing Theory, Advances in Futures and Options Research 7 (1994) 267–311.

[35] P. Zhang, Exotic Options, 2nd Edition, World Scientific, 1998.

[36] J. R. M. Röman, Analytical Finance: Volume I and II: The Mathematics of Equity Derivatives, Markets, Risk and Valuation, Palgrave Macmillan, 2017.

[37] R. Zvan, P. A. Forsyth, K. R. Vetzal, Robust numerical methods for PDE models of Asian options, Journal of Computational Finance 1 (2) (1997) 39–78.

[38] J. E. Ingersoll, Theory of Financial Decision Making, Rowman & Littlefield, 1987.

[39] L.C.G.Rogers, Z.Shi, The Value of an Asian option, Journal of Applied Probability 32 (4) (1995) 1077–1088.

[40] C. Burgard, M. Kjaer, PDE representations of derivatives with bilateral counterparty risk and funding costs, Journal of Credit Risk 7 (2011) 1–19.

[41] A. Agarwal, S. D. Marco, E. Gobet, J. G. López-Salas, F. Noubiagain, A. Zhou, Numerical approximations of McKean anticipative backward stochastic differential equations arising in initial margin requirements, ESAIM: Proceedings and Surveys 65 (2019) 1–26.

[42] M. J. Castro, T. Morales de Luna, C. Parés, Well-Balanced Schemes and Path-Conservative Numerical Methods, in: R. A. a. C.-W. Shu (Ed.), Handbook of Numerical Analysis, Vol. 18 of Handbook of Numerical Methods for Hyperbolic ProblemsApplied and Modern Issues, Elsevier,

2017, pp. 131–175. `doi:10.1016/bs.hna.2016.10.002`.

URL `http://www.sciencedirect.com/science/article/pii/`
`S1570865916300333`

[43] B. Fornberg, Generation of Finite Difference Formulas on Arbitrarily
Spaced Grids, Mathematics of Computation 51(184) (1988) 699–706.